HOW TO USE SANC TO IMPROVE THE PHOTOS MONTE CARLO SIMULATION OF BREMSSTRAHLUNG IN LEPTONIC W-BOSON DECAYS* **

G. Nanava

Lab. of Nuclear Problems, JINR, 141980 Dubna, Russia

and Z. Wąs

H. Niewodniczański Institute of Nuclear Physics
Radzikowskiego 152, 31-342 Cracow, Poland
and
CERN, Theory Division, 1211 Geneva 23, Switzerland

(Received February 4, 2003)

Using the SANC system we study the one-loop electroweak standard model predictions, including virtual and real photon emission, for the decays of the on-shell vector boson, $W \to l\nu_l(\gamma)$. The complete one-loop corrections and exact photon emission matrix element are taken into account. For the phase–space integration, the Monte Carlo technique is used. This provides a useful element, first for the evaluation of the theoretical uncertainty of PHOTOS. Later we analyse the source of the differences between SANC and PHOTOS and we calculate the additional weight, which once installed, improves predictions of PHOTOS simulations. We can conclude that, after the correction of the weight is implemented, the theoretical uncertainty of PHOTOS simulations due to an incomplete first-order matrix element is reduced to below $\frac{\alpha}{\pi}$, for observables not tagging the photon in a direct way, and to 10% otherwise. This is interesting for applications in the phenomenology of the ongoing LEP2 and future LC and LHC experimental studies.

PACS numbers: 12.15.Lk, 13.20.Cz

* Includes material presented at the Cracow Epiphany Conference on Heavy Flavors, Cracow, Poland, January 3–6, 2003.

** Work supported in part by the European Union 5-th Framework under contract HPRN-CT-2000-00149, Polish State Committee for Scientific Research (KBN) grant 2 P03B 001 22, NATO grant PST.CLG.977751 and INTAS N° 00-00313.

1. Introduction

The SANC project of Ref. [1] has several purposes. The intermediate goal is to summarize and consolidate the effort of the last three decades in calculating Standard Model radiative corrections for LEP, in a well organized calculational environment, for future reference. However, it is aimed not only at training young researchers and students, but at some remaining calculational projects for LEP as well. Recently it was used for that purpose in [2].

An important lesson from the LEP experiments [3] is that the desirable way of providing theoretical predictions is in the form of Monte Carlo event generators. This aspect has been taken into account in the development of SANC from an early stage of its development.

The currently available version can construct one-loop spin amplitudes for the decays of the gauge bosons W and Z and of the Higgs boson H. For the moment, SANC features single real-photon emission, in the calculations of the total rate and decay spectra of the $B \to f\bar{f}(\gamma)$ process. The complete spin polarization density matrix of the decaying boson is taken into account as well.

The integration, with the Monte Carlo method, over the three(two)-body final state is done without any approximation (in particular, the small-mass approximation is not used). The program provides MC events with constant weight (unweighted events). The whole system is, therefore, fairly self-contained and complete.

It is of the utmost importance for such a system to reproduce known results precisely; this step of its development was completed in Ref. [2]. Let us turn now to its application: first find an approximation of the relatively large terms missing in PHOTOS [4] for generation of bremsstrahlung in W decay, later install them into this program, and finally verify, again with SANC, that the PHOTOS algorithm for the generation of bremmstrahlung in decays, after modifications, works indeed better.

Our paper is organized as follows: in the next section we recall, from [2], the set of observables chosen for tests and we explain the input parameters used in SANC and PHOTOS. Section 3 is devoted to a discussion of the SANC matrix elements for QED bremsstrahlung. The gauge-invariant part of this matrix element, which is expected to be responsible for the PHOTOS discrepancies with exact matrix element, is removed from SANC first. These terms are approximated by simple formula and installed to a PHOTOS. Section 4 describes comparisons of full SANC with PHOTOS with the new correcting weight introduced. A summary, Section 5, closes the paper.

2. Initialization set-ups for SANC and PHOTOS runs

In the following sections we compare predictions from the programs SANC and PHOTOS. It is essential that the initialization be identical in all cases and close to the physical reality; in particular the following options are set in the two programs:

- In SANC we switch off the EW part of the radiative corrections. The soft/hard photon limit is kept at 0.005 of the decaying particle mass.
- In PHOTOS we switch off the double bremsstrahlung corrections. The soft/hard photon limit is kept at 0.005 of the decaying particle mass. For the generation of the Born-level two-body decays, we use the Monte Carlo generation from SANC.

To visualize the differences (or the agreement) between the calculations, we choose a certain class of (pseudo-)observables, more precisely the one-dimensional distributions, which are quite similar to the ones used in the first tests of PHOTOS reported in [5]. To visualize the usually small differences, we plot ratios of the predictions from the two programs rather than the distributions themselves.

List of observables:

A *Photon energy in the decaying particle rest frame:* this observable is sensitive mainly to the leading-log (*i.e.* collinear) non-infrared (*i.e.* not soft) component of the distributions.

B *Energy of the final-state charged particle:* as the previous one, this observable is sensitive mainly to the leading-log (*i.e.* collinear) non-infrared (*i.e.* not soft) component of the distributions.

C *Angle of the photon with final-state charged particle:* this observable is sensitive mainly to the non-collinear (*i.e.* non-leading-log) but soft (*i.e.* infrared) component of the distributions.

D *Acollinearity angle of the final-state charged particles:* this observable is sensitive mainly to the non-collinear (*i.e.* non-leading-log) and non-soft (*i.e.* non-infrared) component of the distributions.

3. Complete and truncated matrix elements of SANC

The Feynman diagrams for the decay

$$W^{\pm}(Q,\lambda) \to l(p_l,\lambda_l) + \bar{\nu}(p_\nu,\lambda_\nu) + \gamma(k,\sigma) \tag{1}$$

are shown in Fig. 1 (unitary gauge), where (p_l, λ_l) and (p_ν, λ_ν) denote the four-momentum and helicity of the fermion l and neutrino, respectively, (k, σ) is the four-momentum and helicity of the photon, and (Q, λ) the four-momentum and helicity of the W boson. In the notation of Ref. [6], the

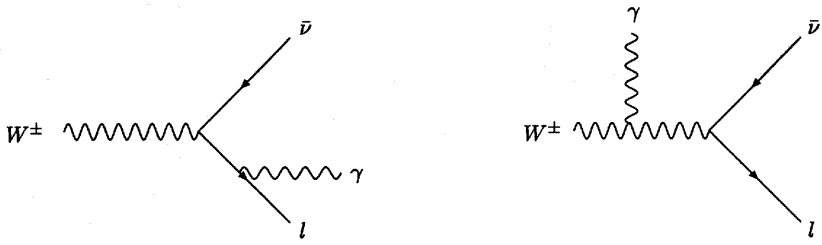

Fig. 1. Feynman diagrams

corresponding parts of spin amplitudes take the form:

$$
\begin{aligned}
M^{\sigma}_{\lambda,\lambda_\nu,\lambda_l}(k,Q,p_\nu,p_l) \;=\; & \left[\frac{Q_l}{2\,k\cdot p_l}b_\sigma(k,p_l) - \frac{Q_W}{2\,k\cdot Q}\left(b_\sigma(k,p_l)+b_\sigma(k,p_\nu)\right)\right] \\
& \times B^{\lambda}_{\lambda_l,\lambda_\nu}(p_l,Q,p_\nu) \\
& + \frac{Q_l}{2k\cdot p_l}\sum_{\rho=\pm} U^{\sigma}_{\lambda_l,\rho}(p_l,m_l,k,0,k,0)B^{\lambda}_{\rho,-\lambda_\nu}(k,Q,p_\nu) \\
& - \frac{Q_W}{2k\cdot Q}\sum_{\rho=\pm}\Big(B^{\lambda}_{\lambda_l,-\rho}(p_l,Q,k)U^{\sigma}_{-\rho,-\lambda_\nu}(k,0,k,0,p_\nu,0) \\
& + U^{\sigma}_{\lambda_l,\rho}(p_l,m_l,k,0,k,0)B^{\lambda}_{\rho,-\lambda_\nu}(k,Q,p_\nu)\Big)\;, \qquad (2)
\end{aligned}
$$

where we have introduced the following notation:

$$
\begin{aligned}
B^{\lambda}_{\lambda_1,\lambda_2}(p_1,Q,p_2) \;&\equiv\; \frac{g}{2\sqrt{2}}\bar{u}(p_1,\lambda_1)\,\widehat{\varepsilon}^{\lambda}_{W}(Q)(1+\gamma_5)\,v(p_2,\lambda_2)\,, \\
U^{\sigma}_{\lambda_1,\lambda_2}(p_1,m_1,k,0,p_2,m_2) \;&\equiv\; \bar{u}(p_1,\lambda_1)\,\widehat{\varepsilon}^{\sigma}_{\gamma}(k)\,u(p_2,\lambda_2)\,, \qquad (3) \\
\delta_{\lambda_1\lambda_2}b_\sigma(k,p) \;&\equiv\; U^{\sigma}_{\lambda_1,\lambda_2}(p,m,k,0,p,m)\,,
\end{aligned}
$$

Q_l and Q_W are the electric charges of the fermion l and the W boson, respectively, in units of the positron charge, $\varepsilon^{\sigma}_{\gamma}(k)$ and $\varepsilon^{\lambda}_{W}(Q)$ denote, respectively, the polarization vectors of the photon and the W boson.

This amplitude can be divided into three gauge-invariant parts:

- Infrared-divergent part:

$$M^{\sigma}_{\lambda,\lambda_\nu,\lambda_l}(k,Q,p_\nu,p_l)^{(\mathrm{a})} = \left[\frac{Q_l}{2\,k\cdot p_l} b_\sigma(k,p_l) - \frac{Q_W}{2\,k\cdot Q}\left(b_\sigma(k,p_l)+b_\sigma(k,p_\nu)\right)\right] B^{\lambda}_{\lambda_l,\lambda_\nu}(p_l,Q,p_\nu)\,. \tag{4}$$

- Collinear-divergent part:

$$M^{\sigma}_{\lambda,\lambda_\nu,\lambda_l}(k,Q,p_\nu,p_l)^{(\mathrm{b})} = \frac{Q_l}{2\,k\cdot p_l}\sum_{\rho=\pm} U^{\sigma}_{\lambda_l,\rho}(p_l,m_l,k,0,k,0) B^{\lambda}_{\rho,-\lambda_\nu}(k,Q,p_\nu)\,. \tag{5}$$

- Finite part :

$$M^{\sigma}_{\lambda,\lambda_\nu,\lambda_l}(k,Q,p_\nu,p_l)^{(\mathrm{c})} = -\frac{Q_W}{2\,k\cdot Q}\sum_{\rho=\pm}\Big(B^{\lambda}_{\lambda_l,-\rho}(p_l,Q,k) U^{\sigma}_{-\rho,-\lambda_\nu}(k,0,k,0,p_\nu,0) + U^{\sigma}_{\lambda_l,\rho}(p_l,m_l,k,0,k,0) B^{\lambda}_{\rho,-\lambda_\nu}(k,Q,p_\nu)\Big)\,. \tag{6}$$

Once the last (finite) term is dropped from the whole amplitude, event distributions produced with SANC and PHOTOS become almost identical; this is shown in Fig. 2, where comparisons of the PHOTOS (truncated SANC) with complete matrix elements are visible on the left-hand (right-hand) part of the figure. This is very encouraging and can be used as a starting point for improving PHOTOS, with the help of some kind of correction weight. We have indeed found that analysing the difference between the complete and truncated matrix elements of SANC such a correction weight δ can be found. One can replace the exact matrix element of SANC with:

$$\sum_{\sigma\lambda\lambda_\nu\lambda_l} |M^{\sigma}_{\lambda,\lambda_\nu,\lambda_l}(k,Q,p_\nu,p_l)^{(a)} + M^{\sigma}_{\lambda,\lambda_\nu,\lambda_l}(k,Q,p_\nu,p_l)^{(b)}|^2\,(1+\delta)\,, \tag{7}$$

where

$$\begin{aligned}\delta &= \frac{\sum_{\sigma\lambda\lambda_\nu\lambda_l}|M^{\sigma}_{\lambda,\lambda_\nu,\lambda_l}(k,Q,p_\nu,p_l)|^2}{\sum_{\sigma\lambda\lambda_\nu\lambda_l}|M^{\sigma}_{\lambda,\lambda_\nu,\lambda_l}(k,Q,p_\nu,p_l)^{(a)} + M^{\sigma}_{\lambda,\lambda_\nu,\lambda_l}(k,Q,p_\nu,p_l)^{(b)}|^2} - 1 \\ &= -8k_0(1-\beta_l\cos\theta)\left(\frac{m_l^2 E_l}{M_W^4(1-m_l^2/M_W^2)(4-m_l^2/M_W^2)} + \frac{2E_l k_0}{M_W^3(1-m_l^2/M_W^2)(4-m_l^2/M_W^2)}\right)\end{aligned} \tag{8}$$

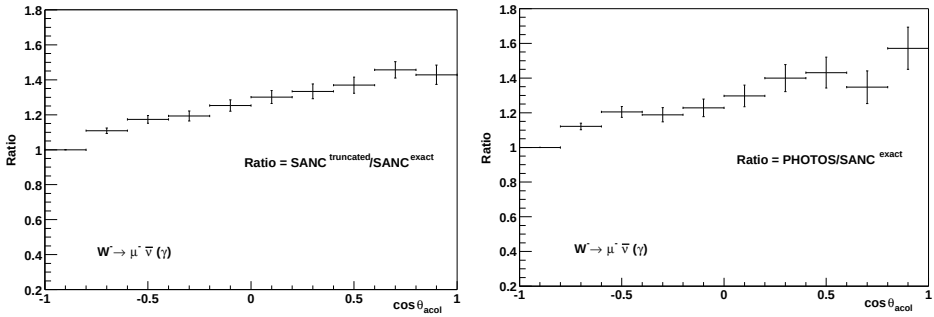

Fig. 2. Comparisons (ratios) of the PHOTOS, truncated SANC and complete SANC predictions for the W decay. Ratio of the $\mu^-\bar{\nu}$ acollinearity distribution from PHOTOS and complete SANC (left-hand side) and ratio of the $\mu^-\bar{\nu}$ acollinearity distribution from truncated SANC and complete SANC (right-hand side) are given. The dominant contribution is of non-leading nature, the observable **D**.

and k_0 denotes the photon energy, while m_l and E_l denote, respectively, the mass and the energy of the fermion l. Finally M_W denotes the mass of the W boson and $\beta_l = \sqrt{1 - m_l^2/E_l^2}$, $\theta = \angle(\vec{p}_l, \vec{k})$ (all kinematical variables defined in the W rest frame). The differences between the results obtained from such approximated matrix elements and those from the complete matrix elements are rather small (see Fig. 3).

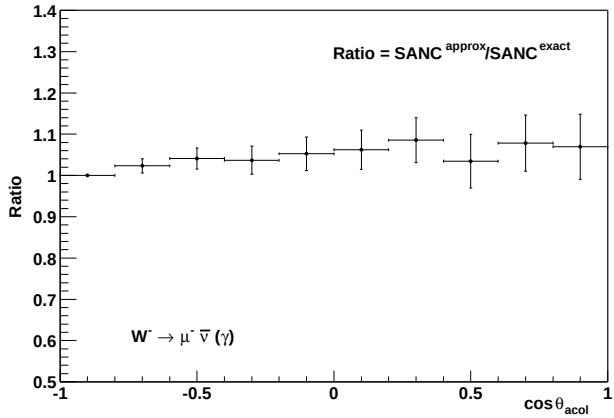

Fig. 3. Comparison (ratio) of the predictions for the W decay from SANC truncated and corrected with the function δ and from the complete SANC. Ratio of the $\mu^-\bar{\nu}$ acollinearity distribution is given. The dominant contribution is of non-leading nature, the observable **D**.

4. Numerical results from the improved PHOTOS

Once our formula (8) was expressed in a simple form, we could rather easily introduce it into PHOTOS as an additional correcting weight, to be activated in the case of leptonic W decays only.

As we can see from Figs. 4, and 5 level of the agreement between the new version of PHOTOS and the complete-matrix-elements calculation of SANC is for all distributions of the types **A, B, C** and **D** at the level of better than 10%. This is true, even in the case of the observable **D**, where the differences, without the correcting weights, were up to 40%.

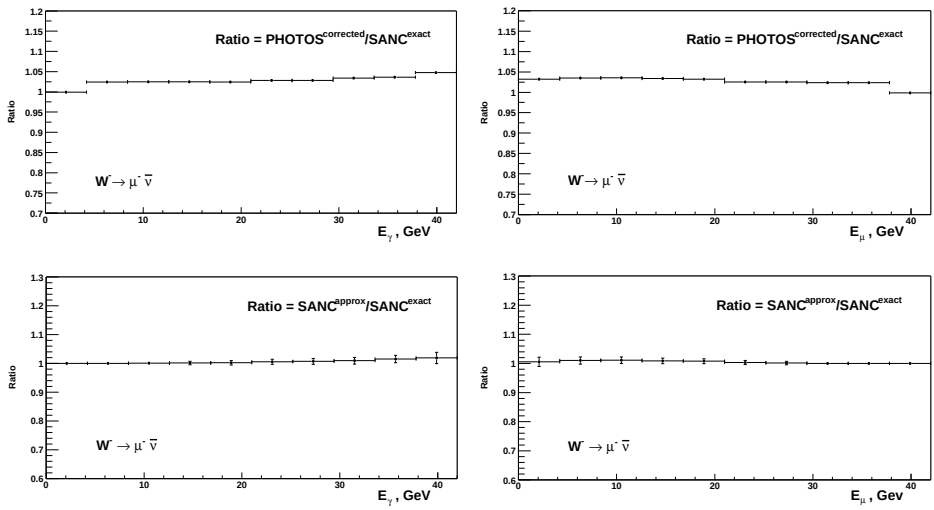

Fig. 4. Comparisons (ratios) of the complete SANC and corrected PHOTOS predictions for the W decay. Observables **A** and **B**: ratios of the photon energy (left-hand side) and muon energy (right-hand side) distributions from the two programs. The dominant contribution is of leading-log (collinear) nature. In the lower part of the plots similar comparisons for the complete SANC and truncated–corrected with δ SANC predictions are given.

Also, as one can see in Fig. 5, comparisons between complete and corrected–truncated versions of SANC give similar patterns of residual differences, as in case of PHOTOS comparisons with the complete matrix elements SANC. This indicates that the approximation used in evaluating formula (8) is at the origin of at least some of the differences between corrected PHOTOS and full-matrix-element calculation, rather than *e.g.* some technical problems related to its Monte Carlo algorithm.

With the correcting weight (8) included, the comparisons of PHOTOS with the "matrix-elements" type calculations improved significantly. The differences were not only largely removed, but also explained as being due to part

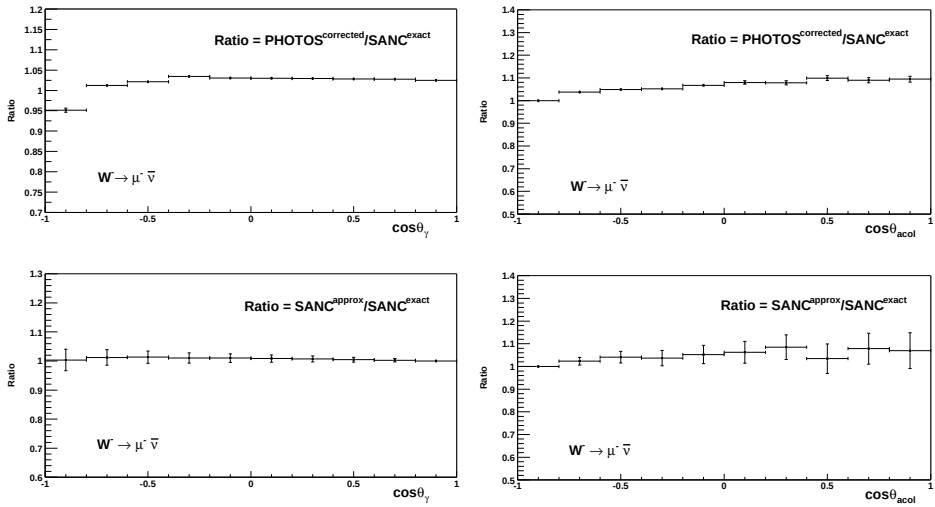

Fig. 5. Comparisons (ratios) of the complete SANC and corrected PHOTOS predictions for the W decay. Observables **C** and **D**: ratios of the photon angle with respect to μ^- (left-hand side) and $\mu^-\bar{\nu}$ acollinearity (right-hand side) distributions from the two programs. The dominant contribution is of infrared non-leading-log nature for the left-hand side plot, and non-infrared non-leading-log nature for the right-hand side one. In the lower part of the plots similar comparisons for the complete SANC and truncated–corrected with δ SANC predictions are given.

of the W–W–γ interaction explicitly missing in older versions of PHOTOS. This indicates that, in future, algorithms of this type can be improved even further, *e.g.* using exponentiation techniques. On the other hand, differences between lower and upper plots of Fig. 4 point toward the limits of the method.

At LEP2, the production and decay of W pairs is now being combined for all four LEP2 experiments, and uncertainties due to bremsstrahlung in W decay are important. PHOTOS is part of the main programs (see *e.g.* YFSWW3 [9]) used in the LEP2 analysis of the W-pair data. The present paper provides a means of estimating the size of the uncertainties from PHOTOS. The correction weight can be switched on and off for that purpose. We hope that, for LEP2 experiments, the updated version of PHOTOS will turn out to be sufficient. However, for higher precision, more sophisticated solutions, *e.g.* as those described in Ref. [10], will have to be used. Finally, let us mention that the W channel is of importance for some studies of the LHC Higgs-discovery potential as well [7,8].

5. Summary

We have successfully tested SANC *versus* PHOTOS in the case of the W decay. We have first checked that once non-leading contributions of SANC related to the W charge are dropped, SANC tends to agree with the results provided by the old version of PHOTOS Monte Carlo. These comparisons convinced us that the deficiencies of PHOTOS are indeed due to missing non-leading terms. The missing terms were then studied analytically within SANC and an approximating correcting weight, for leptonic W decays, was found. Once the weight was installed to the new version of PHOTOS, agreement with respect to complete results of SANC was found. With new correcting weight, the PHOTOS predictions are within 5% (instead of 7% without correcting weight) for the end parts of the spectra affected by the leading-log corrections, but within 5% (instead of 20%) for the angular part of the distributions, where the infrared-induced logarithms dominate. The agreement is now also at the 10% level in the phase–space regions where only non-leading corrections contribute to the matrix elements. This is a significant improvement with respect to old version of PHOTOS, without correcting weight, where differences were up to 40%.

The authors would like to thank D. Bardin, F. Cossutti, S. Jadach and B.F.L. Ward for useful discussions.

REFERENCES

[1] D. Bardin *et al.*, hep-ph/0209297, to be published in ICHEP2002 Proceedings; D. Bardin *et al.*, hep-ph/0202004; D. Bardin, P. Christova, L. Kalinovskaya, *Nucl. Phys. B (Proc. Suppl.)* **116**, 48 (2003).

[2] A. Andonov, S. Jadach, G. Nanava, Z. Wąs, *Acta Phys. Pol. B* **34**, 2665 (2003).

[3] M. Kobel *et al.*, hep-ph/0007180.

[4] E. Barberio, Z. Wąs, *Comput. Phys. Commun.* **79**, 291 (1994).

[5] E. Barberio, B. van Eijk, Z. Wąs, *Comput. Phys. Commun.* **66**, 115 (1991).

[6] S. Jadach, B.F.L. Ward, Z. Wąs, *Phys. Lett.* **B449**, 97 (1999).

[7] E. Richter-Wąs, *Z. Phys.* **C61**, 323 (1994).

[8] ATLAS collaboration, " ATLAS Detector and Physics Performance Technical Design Report", CERN/LHCC/99-15, vol. 2, p. 674.

[9] S. Jadach, W. Placzek, M. Skrzypek, B. F. Ward, Z. Was, *Comput. Phys. Commun.* **140**, 475 (2001).

[10] W. Placzek, S. Jadach, hep-ph/0302065.